Indonesian Journal of Chemical Research

http://ojs3.unpatti.ac.id/index.php/ijcr Indo. J. Chem. Res., 14 (1), 27-39, 2026

Molecular Dynamics Study of Electrolyte Effects on Carbon Electrode in Supercapacitors

Syifa Salsabina[1], Raissa[2], Muttaqin[1], Tirta Rona Mayangsari[1,3*]

[1]Department of Chemistry, Universitas Pertamina, Jl. Teuku Nyak Arief Jakarta Selatan, Jakarta 12220, Indonesia
[2]Research Center for Nanotechnology, National Research and Innovation Agency (BRIN), South Tangerang 15314, Indonesia
[3]Center for Advanced Materials, Universitas Pertamina, Jl. Teuku Nyak Arief Jakarta Selatan, Jakarta 12220, Indonesia
[*]*Corresponding Author: tirta.rm@universitaspertamina.ac.id*

Received: January 2026
Received in revised: April 2026
Accepted: May 2026
Available online: May 2026

Abstract

The demand for efficient and sustainable global energy sources continues to increase alongside technological developments. In this case, the development of electrical energy storage devices, such as supercapcitor, is essential. Supercapacitors have a fairly high capacitance, large power density, fast charging and discharging processes, and good durability. Computational studies through molecular dynamics simulations were conducted to understand the properties and dynamics of a supercapacitor system with activated carbon-based electrodes. This study aims to observe the effect of electrolyte types on the properties of activated carbon as a supercapacitor electrode based on the dynamic movement of electrolyte ions in the system molecular dynamics simulations using Large Scale Atomic/Molecular Massively Parallel Simulator (LAMMPS) software with OPLS-AA force field parameters were carried out to study the supercapacitor system. The variations of electrolyte systems studied include $C_3H_5N_2^+/BF_4^-$, $C_3H_5N_2^+/CH_3COO^-$, and K+/OH- in acetonitrile (ACN) solvent. Simulation results show that the system with $C_3H_5N_2^+/BF_4^-$ electrolyte has the best performance as a supercapacitor system. This is seen from the interface interaction with the electrode and good ion diffusion, the highest ion diffusion coefficient value of $18{,}4\times10^{-11}$ m^2/s, and the highest specific capacitance value of 199,86 $\mu F/cm^2$.

Keywords: supercapacitor, activated carbon, electrolyte, diffusion, molecular dynamics simulation.

INTRODUCTION

The increasing advancement of technology has significantly increased the global demand for efficient and sustainable energy sources. Electricity is essential for various applications, including electronic devices, electric vehicles, household systems, and industrial operations. According to a report from the International Energy Agency (IEA), global electricity demand is expected to continue increasing at an average rate of 3.4% per year until 2026 (IEA, 2024). Therefore, alternative sources of electricity from renewable energy are increasingly being promoted. The drawback of renewable energy sources such as wind and solar is their instability. This necessitates the development of energy storage devices. One widely developed solution is the supercapacitor, an energy storage device that offers the advantages of high energy capacity, high power density, fast charge-discharge processes, and high durability (Shuja et al., 2024).

Supercapacitors utilize the principle of an electrostatic double layer between the electrode and electrolyte surfaces, allowing them to undergo rapid charge-discharge cycles and withstand millions of cycles (Pean et al., 2016). Compared to conventional capacitors, supercapacitors have a higher energy density. This is due to the use of liquid electrolytes and porous electrodes in supercapacitors, which enable the combination of electrostatic and electrochemical mechanisms. Conventional capacitors, on the other hand, utilize only the electrostatic principle of a solid dielectric material (Bueno, 2019). However, supercapacitors have the disadvantage of longer charge-discharge cycle times compared to conventional capacitors and relatively low energy density (Banerjee et al., 2025). Therefore, research into the development of supercapacitors is an important and interesting topic.

The energy storage mechanism in supercapacitors utilizes electrostatic processes through the movement of ions from the electrolyte when a voltage is applied to the electrodes. This

process causes the ions to form an electric double layer between the electrode and electrolyte surfaces (Chaban et al., 2018). This indicates that the performance of supercapacitors as energy storage devices is highly dependent on the interactions between the electrolyte and the electrodes. Material selection and system design are crucial considerations for improving supercapacitor performance (Ionescu & Kovaci, 2024). One type of material widely used as a supercapacitor electrode is carbon-based materials. Carbon was chosen because it has a large surface area, a stable porous structure during charge-discharge cycles, and can facilitate rapid energy transfer. Previous research have demonstrated the broad application of carbon-based electrodes in electrochemical systems due to their favorable electrical conductivity, surface properties, and interfacial characteristics, indicating their potential for energy storage applications (Wahyuni et al., 2021; Fatihah & Setiarso, 2024; Febriyana & Setiarso, 2024). Activated carbon is a type of amorphous carbon known for its high porosity. Activated carbon as a supercapacitor electrode can have a surface area of up to 3000 m^2/g (Theodore et al., 2025).

In addition to electrode material selection, the type of electrolyte must also be considered to improve supercapacitor performance. Electrolytes used in supercapacitors include aqueous electrolytes, organic electrolytes, ionic liquids, and hybrid electrolyte systems. Some examples of liquid electrolytes in supercapacitors include solutions of H_2SO_4, KOH, $EMIM^+/BF_4^-$, imidazolium-based ions in organic solvents, and others. The type of electrolyte is selected by considering the electrode material used, the size and type of ions, the interaction between ions and solvents, concentration, and electrochemical stability (Theodore et al., 2025). The selection of the electrolyte is a crucial factor in supercapacitors because it will affect the energy capacity, performance rate, cycling process, and device durability during use (Xia et al., 2017). Therefore, it is important to have a deep understanding of the interactions that occur between the electrolyte and activated carbon electrodes at the molecular level so that it can optimize supercapacitor performance.

A Molecular Dynamics (MD) simulation is needed to understand the interactions between activated carbon electrodes and electrolyte ions in a supercapacitor system. This allows for a more in-depth analysis of the structural and electrochemical properties of the materials used, and allows for a view of the system dynamics at the molecular level (Y. Wu et al., 2024). This simulation helps optimize supercapacitor electrode design before conducting live experiments. This can reduce research costs because in-depth initial analysis is performed to predict material performance without the need for expensive and time-consuming trials. By understanding interactions at the molecular level through molecular dynamics simulations, supercapacitor systems can be designed with superior properties, such as improved stability, higher conductivity, high capacitance, and optimal energy storage efficiency.

Recent molecular dynamics studies on supercapacitors have mainly focused on conventional ionic liquid electrolytes and ideal carbon models such as graphene-based electrodes. For example, Xu et al. (2023) investigated BMI^+/PF_6^- ionic liquids on MoS_2 electrodes, while Inoe et al. (2020) focused on graphene-based supercapacitors. Although various organic electrolytes have been widely investigated computationally, studies involving amorphous activated carbon electrodes remain relatively limited compared with graphene-based systems. In practical supercapacitor applications, however, activated carbon is more commonly used because of its porous amorphous structure and high surface area. In addition, previous studies rarely emphasized the molecular-level mechanism of electric double layer capacitor (EDLC) formation through detailed electrode-electrolyte interaction analysis (Inoue et al., 2020). Therefore, this study focuses on investigating the EDLC mechanism in activated carbon-based supercapacitors through molecular dynamics simulations by analyzing ion diffusion behavior, electric double layer formation, number density profiles, ion coverage, and specific capacitance. Particular attention is given to the effects of ion size, intermolecular interactions, and ion-solvent solubility on ion mobility and electrochemical performance.

MD simulations were performed using the Large-scale Atomic/Molecular Massively Parallel Simulator (LAMMPS) application. The LAMMPS application was chosen because it is flexible and capable of simulating molecular dynamics with various types of interatomic forces. The analysis carried out was to observe the dynamics of ion movement in the supercapacitor as a form of interaction between the electrolyte and the activated carbon electrode, calculating the diffusion coefficient, and the specific capacitance value of the supercapacitor. The electrolytes used were imidazolium tetrafluoroborate ions ($C_3H_5N_2^+/BF_4^-$), imidazolium acetate ($C_3H_5N_2^+/CH_3COO^-$), and

potassium hydroxide (K^+/OH^-) in acetonitrile (ACN) solvent.

METHODOLOGY

Materials and Instrumentals

The hardware used in this research includes a personal laptop with an AMD Ryzen 5 7530U processor with Radeon Graphics @ 2.00 GHz, 16 GB of RAM, Windows 11, and a server rented from Vast.ai with a 1x RTX 2090 GPU, AMD EPYC 7502 processor, 32/64 CPUs, and 130 GB of RAM. The personal laptop was used to create molecular structures, build systems, and analyze data. The server device was used to run molecular dynamics simulations.

The primary software used in this research is Large-scale Atomic/Molecular Massively Parallel Simulator (LAMMPS) version 29 August 2024 for molecular dynamics simulations. In addition, Avogadro software version 1.2.0 was also used to create the molecular structures of K^+, OH^-, $C_3H_5N_2^+$, $CH3COO^-$, BF_4^-, and acetonitrile (ACN) ions. PACKMOL program version 20.14.3 was used to place the starting points of the molecules in the defined containers. Moltemplate program version 2.22.0 was used to support the force field parameterization input file. The simulation trajectory results were visualized using the OVITO program version 3.11.3.

Methods

The simulation model used in this study is a supercapacitor system using activated carbon electrodes with electrolyte variations in the form of $C_3H_5N_2^+/BF_4^-$, $C_3H_5N_2^+/CH_3COO^-$, and K^+/OH^- ions in ACN solvent. Details of the number of molecules for the electrodes and electrolytes in the simulation model as shown in Table 1 below.

Table 1. Simulation model variations

System Name	Elektrolyte	$N_{cation/anion}$	N_{ACN}
IMI-BF4	$C_3H_5N_2^+$/ BF_4^-	126	1205
IMI-ACE	$C_3H_5N_2^+$/ CH_3COO^-	126	1205
KOH	K^+/ OH^-	126	1205

The force field used is OPLS-AA as a mathematical function and parameter to determine the interaction force and potential energy between molecules in the simulation model. The preparation of the electrolyte model in the form of an ionic solution in ACN solvent began with the creation of the molecular structures of K^+, OH^-, $C_3H_5N_2^+$, CH_3COO^-, BF_4^-, and ACN using the Avogadro program, which were then optimized and saved in .pdb file format. The electrolyte molecules in the IMI-BF4, IMI-ACE, and KOH systems were mixed and distributed in a 50×47.5×44 Å box with the number of molecules according to Table 1 using PACKMOL. The mixture file was converted into a LAMMPS input file with OPLS-AA force field parameters using Moltemplate.

The structure of activated carbon was obtained through a simulation process using the liquid quenching method using LAMMPS (Li et al., 2013). The initial carbon structure before simulation was graphite, a four-layer graphene sheet with an interlayer spacing of 3.35 Å, parameterized by the OPLS-AA force field. This graphite structure was fabricated in a 50×47.5×13.05 Å box. Minimization was then performed with a time step of 0.25 fs. The liquid quenching method began with an equilibration temperature of 300 K under constant energy and volume conditions (NVE ensemble). The system was then heated to 8000 K and held for 2 ps. After melting, the system was rapidly cooled using an exponential cooling rate of $T = 8000e^{-ct}$, where $c = 1.64\times10^{12}$ and t = 2 ps. This caused the system to return to its minimum energy while maintaining the amorphous structure formed during heating. After the electrolyte and electrode models were prepared, the supercapacitor model was created. The activated carbon electrode model was combined with the electrolyte model according to the IMI-BF4, IMI-ACE, and KOH systems using Moltemplate. The dimensions of the supercapacitor system box are 50×47.5×121 Å with periodic boundary along with xyz axis.

Data Analysis

Ion mobility can be evaluated based on the diffusion coefficient, which represents the amount of substance that moves across a unit area per unit time. The diffusion coefficient *(D)* can be determined using the Einstein relation, derived from the slope of the Mean Square Displacement (MSD) curve with respect to time (X. Wu et al., 2005):

$$D = \frac{1}{6} \lim_{t\to\infty} \frac{d}{dt} MSD \qquad (1)$$

In principle, a higher diffusion coefficient indicates that molecules can move more easily within the system. The specific capacitance *(C)* represents the ability of a supercapacitor to store electric charge per unit mass or area. This value reflects how much charge can be stored at the interface between the electrode surface and the electrolyte.

$$\sigma = \frac{Q}{A} \quad (2)$$

$$\Delta V = V_+ - V_- \quad (3)$$

$$C = \frac{\sigma}{\Delta V} \quad (4)$$

Specific capacitance is the system's ability to store electrical charge per unit area of the electrode. A higher capacitance value indicates a greater energy storage capacity in the supercapacitor. According to equation 2, 3, and 4, σ denotes the surface charge density, Q is the total charge on the electrode, and A is the surface area of the electrode in contact with the electrolyte. ΔV represents the potential difference, where V_+ is the potential at the cathode and V_- is the potential at the anode. C corresponds to the specific capacitance (Inoue et al., 2020). In equilibrium molecular dynamics simulations, structural and transport properties are obtained through statistical sampling over sufficiently equilibrated trajectories. Therefore, the calculated properties in this work were evaluated from time-averaged data collected continuously during the production stage.

RESULTS AND DISCUSSION

System Parameter Validation

This study uses the OPLS-AA (Optimized Potentials for Liquid Simulations – All Atom) force field as system parameters obtained from the Force Field Documentation on Moltemplate by Andrew Jewett. The parameters in this version of OPLS-AA were developed and optimized from information in a research paper by Jorgensen et al. in 2024 (Jorgensen et al., 2024). The OPLS-AA force field was chosen in this study because it contains the information needed for molecular dynamics simulations, especially small organic molecules in liquid form, making it suitable for observing electrolyte dynamics in supercapacitor simulations. Parameters and mathematical expressions that define the potential energy of the system in terms of atomic positions include atomic charge, atomic mass, pair coefficient, bond coefficient, angle coefficient, dihedral coefficient, as well as Lennard-Jones interactions and electrostatic interactions. Furthermore, OPLS-AA contains all-atom parameters that have been used and developed in large-system simulations that require lengthy runs and accurate calculations for electrostatic forces (Zangi, 2018).

Validation of the system parameters aims to ensure that the system and simulation method adequately represent the physical and chemical behavior of the actual system. This step is crucial for more accurate simulation results, allowing them to serve as a reference for observing the influence of electrolyte type on supercapacitor systems, as a preliminary, in-depth analysis prior to experimentation. Simulation results from a previous study on the ionic liquid mixture BMIM-BF4 in ACN served as a reference for validating the OPLS-AA force field used to model the supercapacitor system (X. Wu et al., 2005). In this validation stage, the density and diffusion coefficients were systematically compared with the molecular dynamics results reported by Wu et al. (2005). The comparison focused on evaluating whether the simulation trends and electrolyte behavior obtained in this work were consistent with the reference study. This step was conducted through NPT simulations of the imidazolium-BF4 mixture in ACN with varying imidazolium-BF4 mole fractions of x_1 = 0.2; 0.4; and 0.8. The system was created in a 40×40×40 Å simulation box with details of the number of molecules as in Table 2 below.

Table 2. Composition of the mixture systems used for parameter validation simulations

x_1	$N_{imidazolium}$	N_{BF4}	N_{ACN}
0.203	52	52	204
0.398	102	102	154
0.797	204	204	52

The mixture system simulation was performed starting with the minimization phase, followed by equilibration using the NVT ensemble for 50 ps and the NPT ensemble for 75 ps. After the system's energy potential tended to converge during the simulation, indicating that the system was stable and well-equilibrated, the simulation phase could proceed. Molecular dynamics simulations to obtain the density *(ρ)* and diffusion coefficient *(D)* of the system were performed using the NPT ensemble with a time step of 1 fs for 2 ns, with the temperature and pressure held constant at 300 K and 1 barr, respectively. During the simulation, the volume of the mixture system varied to adapt to the real-world conditions based on the parameters used.

Table 3. NPT simulation results of mixed system at T = 300 K, P = 1 barr

x_1		ρ (g/cm^3)	Diffusion Coefficient (10^{-11} m^2/s)			
			D_+	D_-	D_2	D
0,2	This work	1,091	90,1	98,0	108,6	102,4
	Reference	0,989	18,2	22,5	73,6	62,8
0,4	This work	1,216	44,4	45,6	58,3	49,9
	Reference	1,087	5,5	5,6	21,1	14,9
0,8	This work	1,334	32,5	35,8	38,2	34,0
	Reference	1,171	1,4	1,5	5,6	2,3

*This work used a mixture of imidazolium-BF_4 in ACN, while the reference (X. Wu et al., 2005) used a mixture of BMIM-BF_4 in ACN. ρ is the density of the mixture after NPT simulation. D_+, D_-, D_2, and D respectively represent the diffusion coefficients of cations (imidazolium or BMIM), anions (BF_4^-), ACN, and the mixture of imidazolium-BF_4 or BMIM-BF_4 + ACN.

Table *3* shows that the density and diffusion coefficient of the simulated mixture system in this work have the same trend as the reference.

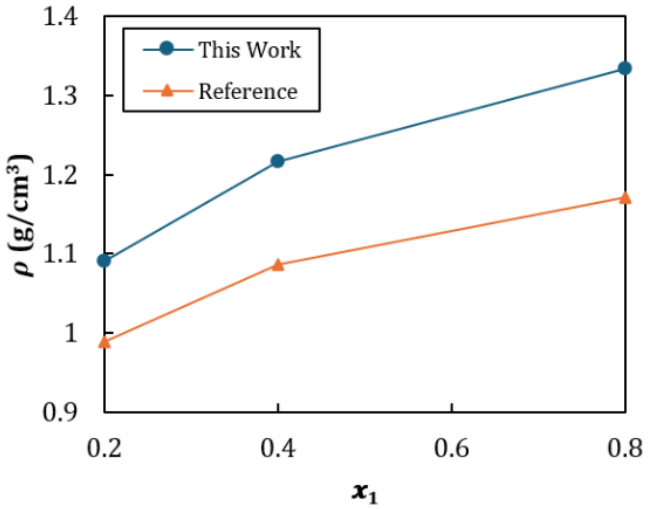

Figure 1. Graph of the density of imidazolium-BF_4 + ACN simulated in this work and the density of BMIM-BF_4 + ACN simulated in the reference

According to Figure 1, the densities of the simulated mixtures in this work and the reference have absolute relative deviation (ARD) values for the mixture systems with x_1 = 0.2; 0.4; and 0.8 of 10.3%, 11.7%, and 13.9%, respectively. The ARD value limit indicating good accuracy between simulation and experimental results is <7% (X. Wu et al., 2005). The difference in density and ARD values of >10% in this work and the reference is due to the different cation molecules: imidazolium is smaller than BMIM, resulting in a higher mixture density due to the smaller system volume. Therefore, the system parameters can still be considered valid because they have the same trend and are quite close to the reference. Density values tend to increase with increasing x_1, both in this work and the reference.

The diffusion coefficient values of D_+, D_-, D_2, and D in this work and the reference also show a similar trend. This can be seen in Figure 2, which shows that the diffusion coefficient values decrease with increasing x_1.

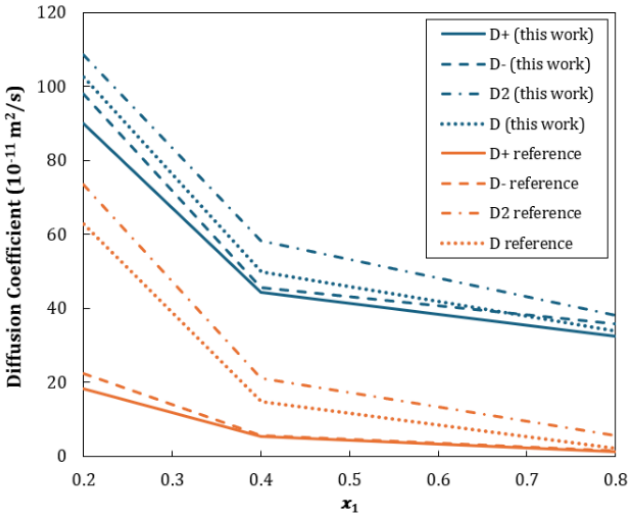

Figure 2. Graph of diffusion coefficients of cations, anions, ACN, and mixturesin this work and the reference

The difference in diffusion coefficient values between this work and the reference is due to the different molecular sizes of the cations, that is imidazolium being smaller than BMIM. This causes imidazolium to diffuse more easily, resulting in a larger diffusion coefficient. The density and diffusion

coefficient graph trends of the simulation results in this work show results similar to those of the reference (X. Wu et al., 2005), that the larger the mole fraction, the higher the density and the lower the diffusion coefficient. Therefore, the validation stage of the OPLS-AA force field can be said to be good and suitable for use as a parameter in creating a supercapacitor model in this study.

Electrolyte Dynamics Analysis in Supercapacitor Systems

Preliminary trial simulations were conducted to evaluate the equilibration behavior and stability of the systems before the final production simulation was performed. Based on the trajectory visualization results, and the total energy of the systems remained relatively constant during the production stage, indicating stable equilibrium conditions. Therefore, the 10 ns simulation period was considered sufficient to analyze the electrolyte dynamics and EDL formation behavior in the present systems. Electrolyte dynamics were analyzed based on the simulation trajectory video of the IMI-BF4, IMI-ACE, and KOH systems for 10 ns in the NVT ensemble, namely when the temperature is 300 K. This analysis aims to observe the dynamics of ion movement regarding their interaction with activated carbon electrodes charged with ±0.01 e (1 e = 1.602×10^{-19} C) for each carbon atom on the cathode and anode. The cathode is on the right marked (+), while the anode is on the left marked (-). In supercapacitors, energy storage occurs through the formation of EDL on the electrode and electrolyte surface (Neto & Fileti, 2018). The EDL structure formed during the simulation can provide an understanding of the performance of each electrolyte. From this analysis, an evaluation can be made regarding the formation of EDL which determines the storage performance and charging speed in the supercapacitor system.

Figure 3 shows a visualization of the trajectory of ion distribution changes in the IMI-BF4 system during the simulation.

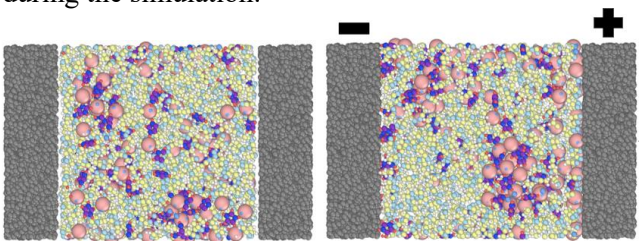

Figure 3. Visualization of the IMI-BF4 system simulation for 10 ns

At t = 0 ns, the ions are still evenly distributed within the ACN solvent. Then, at t = 10 ns, some ions begin to accumulate near the electrode surface. Others remain in the center of the electrolyte system, either dispersed as individual anions and cations or aggregating to form large molecules. In the IMI-BF4 system, BF_4^- anions diffuse toward the cathode, and imidazolium+ cations move toward the anode. This indicates the formation of the EDL structure typical of supercapacitor systems. EDL formation occurs immediately within the first few picoseconds (ps) of the simulation. Significant ion accumulation occurs starting around 4-5 ns, and the EDL appears quite regular on the electrode surface (Figure 4).

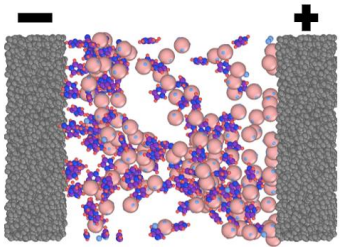

Figure 4. Visualization of the ion distribution of the IMI-BF4 system at t = 4 ns, the ACN molecules are transparent

Then, Figure 5 shows a visualization of the ion distribution changes in the IMI-ACE system during a 10 ns simulation.

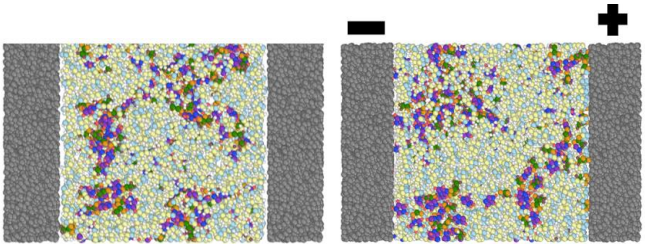

Figure 5. Visualization of the IMI-ACE system simulation for 10 ns

The IMI-ACE system also exhibits EDL formation similar to that of IMI-BF4. $Acetate^-$ anions tend to accumulate at the cathode, while $imidazolium^+$ cations move toward the anode, indicating the formation of an EDL structure. EDL formation occurs immediately within the first few picoseconds (ps) of the simulation. However, compared to IMI-BF4, ion accumulation in the IMI-ACE system appears less dense. EDL formation becomes significant starting around 8-9 ns, as seen in Figure 6.

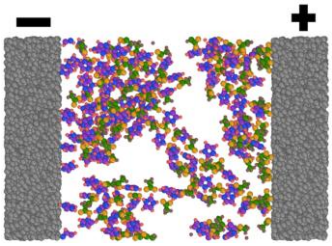

Figure 6. Visualization of the ion distribution of the IMI-ACE system at t = 8 ns, the ACN molecules are transparent

Furthermore, the trajectory of the KOH system during the 10 ns simulation can be seen in Figure 7 below.

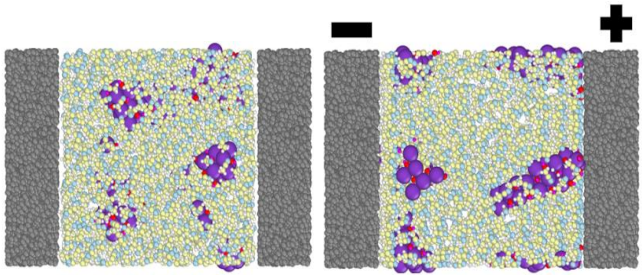

Figure 7. Visualization of the KOH system simulation during 10 ns

Unlike the previous two systems, the KOH system did not exhibit clear EDL formation. The K^+ cations and OH^- anions did not separate into freely dissolved ions in solution, but instead formed KOH molecules due to their low solubility in the ACN solvent. This prevented the anions and cations from diffusing toward the cathode and anode, indicating that the KOH system was unable to form EDLs for energy storage. EDL formation in the KOH system was not observed even up to t = 10 ns (Figure 8).

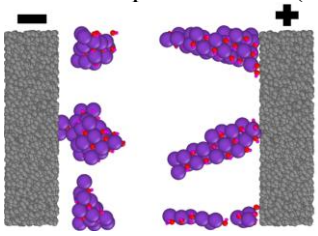

Figure 8. Visualization of ion distribution in the KOH system at t = 10 ns, the ACN molecules are transparent

The KOH system was intentionally included as a comparative electrolyte model to investigate the effect of poor ion-solvent compatibility on EDL formation and ion transport behavior. The observed aggregation behavior is consistent with the known low solubility of KOH in aprotic organic solvents such as ACN. Similar electrolyte behavior has also been reported in previous computational studies, where poor ion-solvent compatibility in organic electrolytes reduced ion dissociation and limited ion transport near electrode surfaces, resulting in weaker electric double layer formation and lower electrochemical performance (Inoue et al., 2020).

To quantify the visualization of EDL formation in each system, we analyzed the percentage ion coverage on the electrode surface. To obtain the ion surface area, each ion molecule was assumed to be spherical.

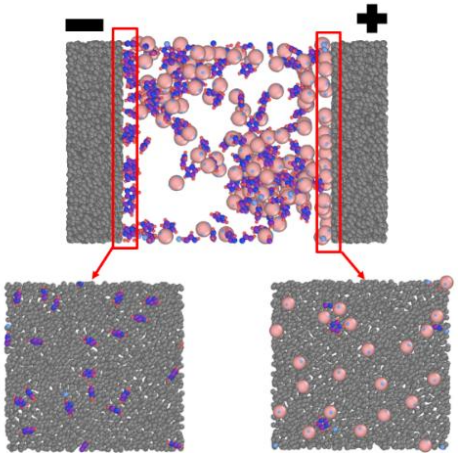

Figure 9. Visualization of ion coverage for the IMI-BF4 system at t = 10 ns

Figure 9 shows a visualization of the ion coverage directly attached to the electrode surface in the first layer for the IMI-BF4 system. The BF_4^- anion has coverage percentage of 10.62%, and the $imidazolium^+$ cation has coverage percentage of 14.06%. Then, Figure 10 shows a visualization of the ion coverage directly attached to the electrode surface in the first layer for the IMI-ACE system. The acetate- anion has a coverage percentage of 9.36%, and the $imidazolium^+$ cation has a coverage percentage of 6.03%.

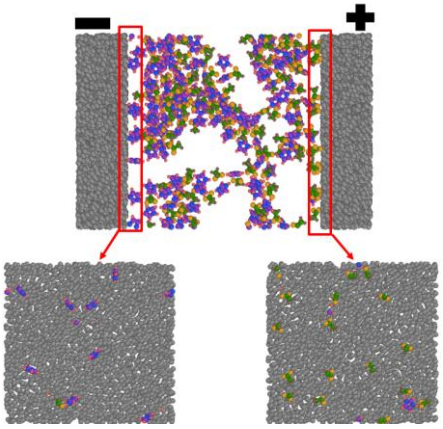

Figure 10. Visualization of ion coverage for the IMI-ACE system at t = 10 ns

The coverage percentages for both cations and anions in the IMI-BF4 system are higher than those in the IMI-ACE system. This supports the qualitative analysis of electrolyte dynamics based on video trajectory simulation results, which demonstrates that EDL formation is superior in the IMI-BF4 system compared to the IMI-ACE system. However, for the KOH system, ion coverage percentages on the electrode surface were not calculated because the ions do not separate to form EDL.

As a form of system stability verification before the main simulation for 10 ns, a number density profile analysis was first performed at the equilibration stage for 2 ns (Figure 11). The ion distribution in the z-axis direction indicates a system condition that has stabilized at a temperature of 300 K.

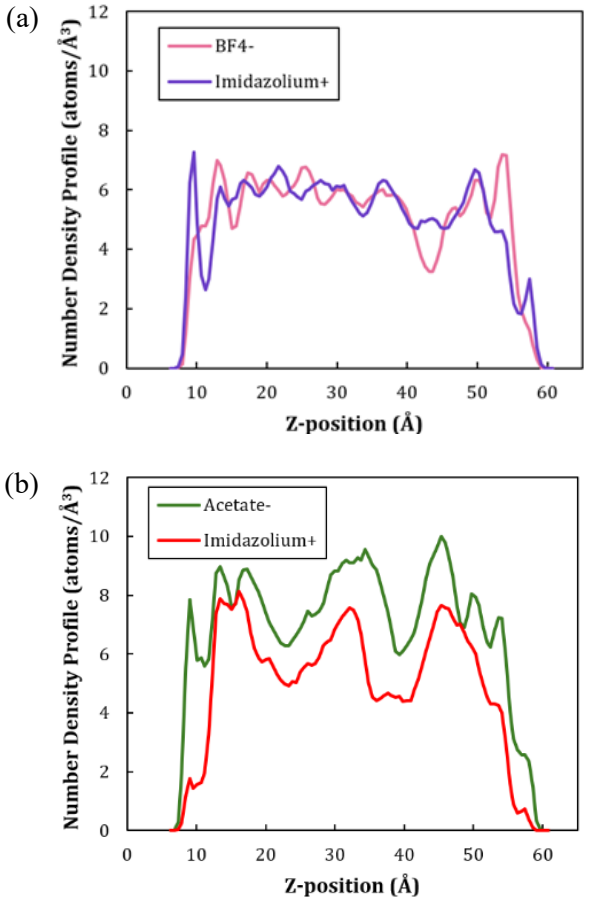

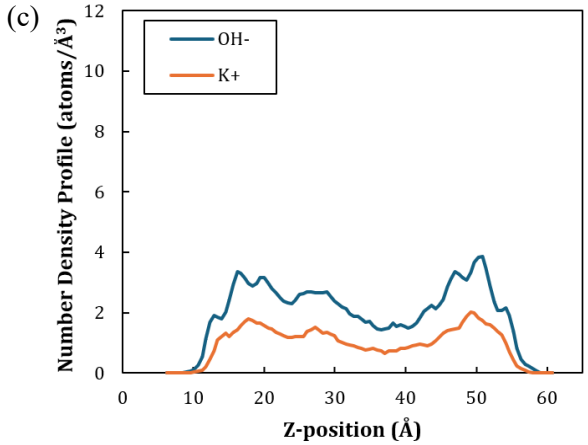

Figure 11. Graph of ion number density profile at the equilibration stage for 2 ns for the IMI-BF4 (a), IMI-ACE (b), and KOH (c) systems

According to Figure 11, each ion pair in the three systems is evenly distributed between the cathode and anode. The density values (y-axis) are relatively symmetrical on both sides and are in a lower range compared to the number density profile graph during the production simulation stage in Figure 12. This indicates that during the equilibration stage, the three systems have not yet accumulated ions near the electrode surface, thus preventing the formation of an EDL structure. The electrolyte system after equilibration, with ions distributed between the anode and cathode, is an ideal initial condition before the electrodes are charged during the 10 ns simulation charge cycle. Furthermore, this condition can also be used as a representation of the state during the discharge cycle.

Next, the number density profile analysis for the 10 ns simulation during the production stage can be seen in Figure 12 Simply put, the charge distribution model at the electrode-electrolyte interface in an EDLC supercapacitor is based on Helmholtz layer theory. This layer forms because the charge on the electrode attracts ions with opposite charges from the electrolyte and repels ions with the same charge. This attractive interaction results in the formation of a thin layer of opposite charge near the electrode surface, known as the EDL (Helmholtz, 1879). Based on the number density profile distribution, the EDL structure can be divided into three layers. First, Inner Helmholtz Plane (IHP), is a layer of ions located 5 Å from the electrode surface and usually in direct contact with no solvent between them. Second, Outer Helmholtz Plane (OHP), is a layer of ions located 5-10 Å from the electrode surface. Third, diffusion layer, is located >10 Å from the electrode surface (Xu et al., 2023). Therefore, ions that do not directly

adhere to the electrode surface are still part of the EDL as long as they are under the influence of the electrode's electric field.

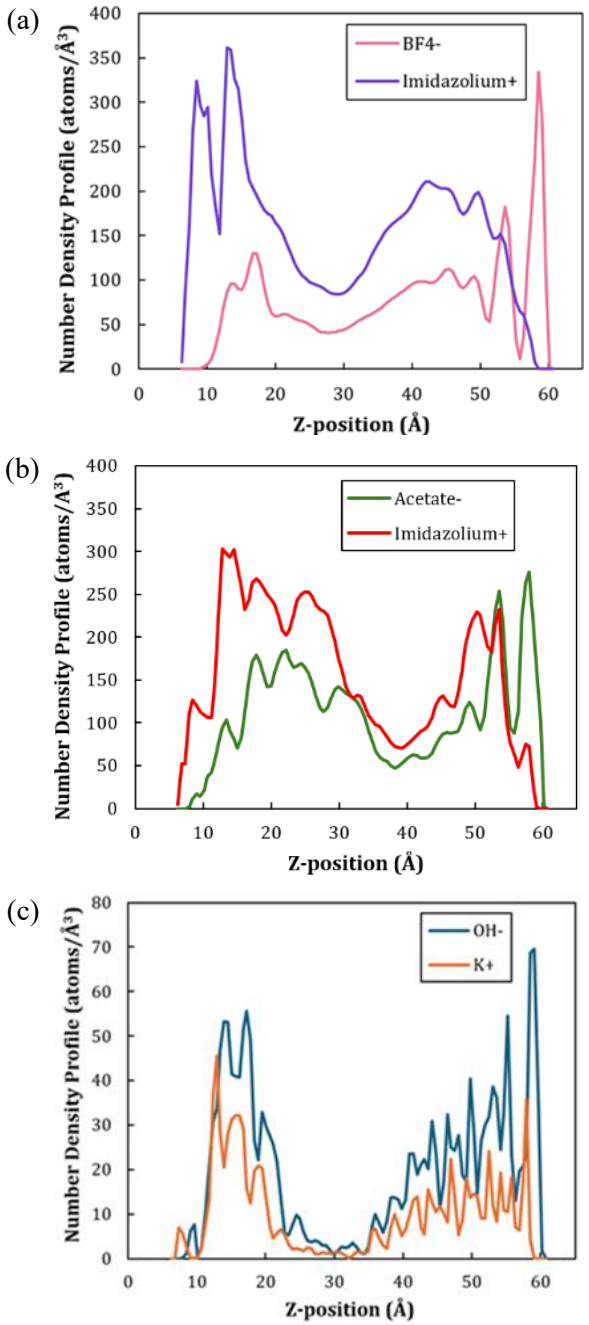

Figure 12. Graph of ion number density profile against the position in the z-axis during the simulation for the IMI-BF4 (a), IMI-ACE (b), and KOH (c) systems

Based on Figure 12(a), the density profile of the ions in the IMI-BF4 system shows a clear accumulation around the electrode surface. The density profile of the imidazolium+ cation has a sharp peak on the anode surface, namely at z-position 6-10 Å. This area indicates the first EDL that directly attaches to the anode surface. Meanwhile, the BF_4^- anion also shows a density profile with a sharp peak on the cathode surface at the first EDL, namely at z-position 56-60 Å. This indicates the formation of a good and symmetric EDL structure for the IMI-BF4 system. In addition, it is also seen that imidazolium$^+$ and some BF_4^- tend to form the second EDL, namely at z-position 10-16 Å and 51-56 Å, respectively.

The IMI-ACE system also exhibits ion accumulation at the electrode, but with lower intensity and regularity than the IMI-BF4 system, as seen in Figure 12(b). The imidazolium$^+$ cation density profile peaks quite low at z-position 6-11 Å, the first EDL. Then, several high and broad peaks are observed up to the z-position of approximately 32 Å. Meanwhile, the acetate- anion density profile forms a peak at z-position 56-60 Å, the first EDL. In the IMI-ACE system, each peak for the cation and anion regions is accompanied by a peak of nearly the same height for the oppositely charged ion. This indicates that the cations and anions in IMI-ACE tend to interact more strongly than the ion-electrode interactions, resulting in less diffusion than in the IMI-BF4 system. This may be due to the hydrogen bonding between the H atoms in the imidazolium ring and the O atoms in the carboxylate group of acetate.

In Figure 12(c) for the KOH system, no significant peaks are observed near the electrode. Both ion types exhibit a diffuse distribution without any clear ion accumulation toward the electrode. For each K^+ cation peak near the anode, an OH^- anion peak is also observed in that area, and vice versa. This supports the previous trajectory visualization results, which showed that K^+ and OH^- do not dissociate effectively in ACN, but instead form KOH molecules due to their low solubility in the ACN solvent.

According to the electrolyte dynamics analysis of the supercapacitor system, which focused on the electrode-electrolyte interface interaction, from video trajectories, percentage coverage, and number density profiles, the IMI-BF4 system exhibited the most stable and regular EDL formation among the investigated electrolytes. The EDL formation behavior also shows that ions in the IMI-BF4 system diffuse most rapidly toward the electrode compared to the IMI-ACE and KOH systems. Similar behavior was also reported by Chaban et al. (2018), who observed that ion size and electrolyte-electrode interactions strongly influence ion structuring and EDL formation in ultracapacitor systems. Several factors can influence this, including ion structure and size, charge distribution, the presence of hydrogen

bonds or other interactions between ions or ions and solvents, among others. The KOH system that does not form an EDL can also serve as a comparative electrolyte model, indicating that the simulation parameters and methods align with the theory that KOH is insoluble in ACN. To strengthen the results of the electrolyte dynamics analysis, a quantitative analysis was performed by calculating the diffusion coefficient.

Analysis of Diffusion Coefficient

The diffusion coefficient (D) value is a parameter that represents the ability of ion molecules or solvents to move within a supercapacitor system. From this value, the supercapacitor performance can be determined based on the speed of EDL formation and the charging efficiency seen from the ionic conductivity factor. The higher the D value, the better the mobility of the molecules in diffusing in the electrolyte. Analysis of the diffusion coefficient value was carried out on cations (D_+), anions ($D\_$), and ACN as a solvent (D_{ACN}). Based on the simulation results of the IMI-BF4, IMI-ACE, and KOH systems, the diffusion coefficient values obtained are shown in Table 4 below.

Table 4. Diffusion coefficient values from supercapacitor system simulations

System	Diffusion Coefficient (10^{-11} m^2/s)		
	D_+	$D\_$	D_{ACN}
IMI-BF4	16,1	18,4	81,5
IMI-ACE	2,47	2,63	72,0
KOH	0,64	0,69	195,2

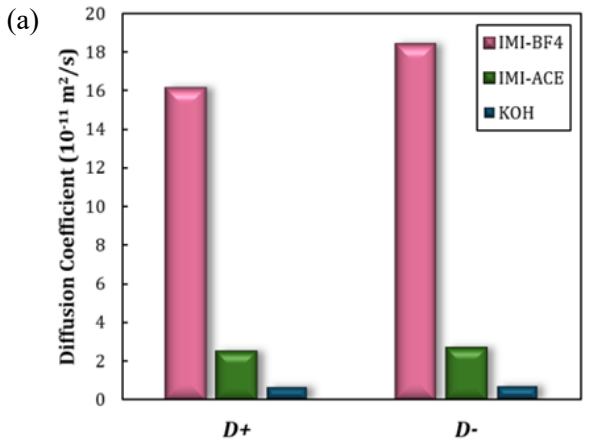

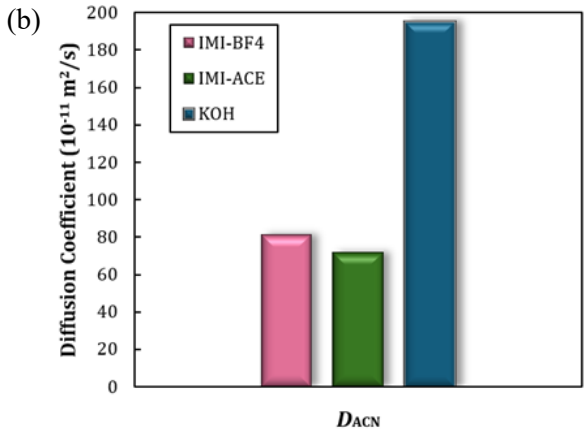

Figure 13. Graph of cation and anion diffusion coefficient values (a), and ACN (b) from supercapacitor system simulations.

Based on Figure 13(a), the diffusion coefficients D_+ and $D\_$ of the IMI-BF4 system are the highest compared to the IMI-ACE and KOH systems. This indicates that the imidazolium$^+$ cation and BF_4^- anion have high mobility or diffusion in the ACN solvent in the supercapacitor system, which is in accordance with the results of the electrolyte dynamics analysis based on the previous trajectory visualization. Judging from its ion structure, the BF_4^- anion has a tetrahedral molecular geometry so it is symmetrical. In addition, BF_4^- is classified as a small and simple ion that cannot form hydrogen bond interactions with other molecules, making it easy to diffuse in polar organic aprotic solvents such as ACN (Rui et al., 2020). On the other hand, the imidazolium$^+$ cation has an aromatic ring so that there is a delocalization of the charge distribution evenly throughout the ring with π bonds. This causes the imidazolium$^+$ to have a less strong attraction to ACN so that it can still move freely in the electrolyte system. The ionic conductivity of the ions in this system can be considered quite good. Therefore, the IMI-BF4 system demonstrated the most rapid and efficient EDL formation compared to the other two systems.

Meanwhile, the IMI-ACE system had significantly lower D_+ and $D\_$ values than IMI-BF4, even though the solvent and cation were the same. This drastically reduced ion mobility is due to the ion-ion interaction between imidazolium$^+$ and acetate-. The acetate$^-$ anion has an O atom in the carboxylate group, which readily forms a strong interaction with the imidazolium$^+$ cation. The O atom in acetate$^-$ can act as a hydrogen bond acceptor, and the H atom bonded to the N in the imidazolium ring is a strong hydrogen bond donor. This makes ion-ion interactions more likely than ion-electrode interactions, resulting in strong attraction between cations and anions,

making it difficult for them to diffuse toward the anode and cathode. Furthermore, weak interactions can also form between acetate- and ACN due to ion-dipole forces. Thus, the anions and cations in the IMI-ACE system tend to form ion pairs, lowering the diffusion coefficient and slowing EDL formation.

The KOH system has very low D_+ and D_- values, indicating that its ions cannot diffuse well as an electrolyte in a supercapacitor system. This proves the previous analysis of electrolyte dynamics based on video trajectories and number density profiles which show that K^+ and OH^- ions cannot dissolve in ACN so that its ionic conductivity is poor. Based on Figure 13(b), the ACN diffusion coefficient value in the KOH system is very high compared to the IMI-BF4 and IMI-ACE systems. This means that ACN in the KOH system is very active in moving in the system because it does not solvate K^+ and OH^- ions well. Therefore, limited ion mobility causes no EDL formation in the KOH system. In contrast, the ACN diffusion coefficient value in the IMI-BF4 and IMI-ACE systems is neither too low nor too high, indicating that ACN as a solvent can facilitate ion movement effectively to increase ion diffusion.

The higher diffusion coefficients observed for the IMI-BF4 system are consistent with previous reports indicating that tetrafluoroborate-based electrolytes exhibit favorable ion mobility and efficient EDL formation due to their relatively small and symmetric ion structure (Chaban et al., 2018). Similar diffusion behavior has also been reported in previous molecular dynamics studies of ionic liquid-based supercapacitor electrolytes, where electrolyte systems with weaker ion pairing and more favorable ion-solvent interactions exhibited higher ion mobility and faster diffusion behavior near electrode surfaces (Burt et al., 2016). The reported diffusion coefficients were in the same order of magnitude as this work (1-100×10^{-11} m²/s). Correspond behavior was observed in the this study, where the IMI-BF4 system exhibited higher diffusion behavior and more stable EDL formation compared with the IMI-ACE and KOH systems.

Analysis of Specific Capacitance

As the main parameter that directly assesses the performance of a supercapacitor system, the specific capacitance *(C)* value describes the system's ability to store electrical charge per unit electrode area. This analysis aims to compare supercapacitor performance based on the *C* value for the IMI-BF4, IMI-ACE, and KOH systems. In principle, the higher the *C* value, the greater the energy density that can be stored by the supercapacitor system. This value will be proportional to the ease of forming the EDL system. Based on calculations from the simulation results with a charge of ±0.01 e, the voltage difference *(ΔV)* in the system was obtained as 0.1 V. The *C* value of the simulated supercapacitor system can be seen in Table 5 below.

Table 5. Specific capacitance values from supercapacitor system simulations

System	Specific Capacitance (μF/cm²)
IMI-BF4	199,86
IMI-ACE	154,85
KOH	130,44

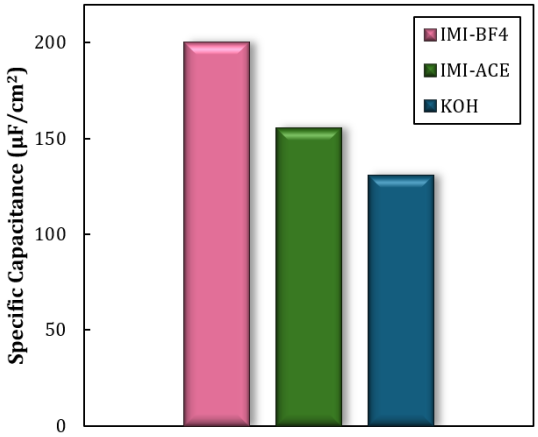

Figure 14. Graph of specific capacitance values from supercapacitor system simulations

Based on the *C* values in Table 5 and the trend in Figure 14, the IMI-BF4 system has the best supercapacitor performance, with the highest *C* value of 199.86 μF/cm², followed by the IMI-ACE system at 154.85 μF/cm², and the KOH system at 130.44 μF/cm². This trend in *C* values is consistent with the results of previous analyses, thus supporting each other, from the analysis of electrolyte dynamics, diffusion coefficient values, to system thermodynamics. IMI-BF4, the system with the best supercapacitor performance, boasts rapid ion diffusion and a uniform density profile distribution around the electrode surface. Trajectory visualization, number density profiles, and diffusion coefficient values demonstrate the formation of a neat EDL in a relatively short time. Thermodynamic analysis also indicates that the IMI-BF4 system favors ion diffusion within the electrolyte.

Previous molecular dynamics investigations of ionic liquid-based EDLC systems demonstrated that capacitance behavior is closely associated with the organization and rearrangement of ions at the

electrode surface during charging processes (Noh & Jung, 2019). The study showed that stable ionic layer formation and effective charge compensation at the electrode–electrolyte interface contribute significantly to improved electrochemical performance. Consistent with these findings, this study shows that the IMI-BF4 system produced the most ordered EDL structure and the highest specific capacitance among the investigated electrolytes, whereas the IMI-ACE and KOH systems exhibited less effective interfacial ion organization and lower capacitance performance.

Confirmed by the specific capacitance values, the IMI-BF4 system is superior to the IMI-ACE and KOH systems for supercapacitor applications in this simulation. In contrast, the KOH system exhibited poor supercapacitor performance due to the low solubility of KOH in ACN, which limited ion dissociation and hindered effective electric double layer (EDL) formation. This study emphasizes the molecular-level mechanism of EDLC formation in amorphous activated carbon electrodes, which are representative of practical supercapacitor materials. The novelty of this work lies in the comprehensive investigation of how ion size, intermolecular interactions, ion-solvent solubility, and electrolyte-electrode interactions influence ion diffusion behavior, EDL formation, and charge storage performance under identical simulation conditions. Therefore, the analysis and trends obtained from these molecular dynamics simulations can serve as an important preliminary approach for future experimental design and electrolyte selection in improving activated carbon-based supercapacitor performance.

CONCLUSION

Molecular dynamics study analysis on the effect of $C_3H_5N_2^+/BF_4^-$, $C_3H_5N_2^+/CH_3COO^-$, and K^+/OH^- electrolytes on the properties of carbon electrodes in supercapacitors has produced several conclusions. First, based on the analysis of electrolyte dynamics in the supercapacitor system that focuses on the interaction of the electrode-electrolyte interface, both from video trajectories, % coverage, and number density profiles, it shows that the IMI-BF4 system has the most optimal ion movement dynamics, with fast and structured EDL formation on the surface of the activated carbon electrode. The IMI-ACE system shows slower and less regular EDL formation than IMI-BF4. Meanwhile, the KOH system does not show clear EDL formation due to the low solubility of K^+ and OH^- ions in ACN solvent. Second, the diffusion coefficient values of D_+ cations for the IMI-BF4, IMI-ACE, and KOH systems are respectively 16.1×10^{-11}; 2.47×10^{-11}; 0.64×10^{-11} m^2/s, while the diffusion coefficients of D_- anions for the three systems are respectively 18.4×10^{-11}; 2.63×10^{-11}; 0.69×10^{-11} m^2/s. These results indicate that the electrolyte with the IMI-BF4 system has better ionic conductivity than IMI-ACE and KOH for the supercapacitor system because it is easier to diffuse. Third, regarding the specific capacitance *(C)* value. Based on the simulation results, the *C* values for the IMI-BF4, IMI-ACE, and KOH systems are respectively 199.86; 154.85; and 130.44 $\mu F/cm^2$. These results show that the supercapacitor with the IMI-BF4 system electrolyte has the highest charge storage capacity compared to the IMI-ACE and KOH systems.

ACKNOWLEDGMENT

This research was supported by Universitas Pertamina through UPERESEARCH 2025 grant for the facilities and support provided during the research process. I would like to thank M. Hasbi Ar-Raihan, S.Si for the helpful suggestions that helped complete this research.

REFERENCES

Banerjee, S., Mordina, B., Sinha, P., & Kar, K. K. (2025). Recent Advancement of Supercapacitors: a Current Era of Supercapacitor Devices Through the Development of Electrical Double Layer, Pseudo and Their Hybrid Supercapacitor Electrodes. *Journal of Energy Storage*, 108, 115075.

Bueno, P. R. (2019). Nanoscale Origins of Super-Capacitance Phenomena. *Journal of Power Sources*, 414, 420–434.

Burt, R., Breitsprecher, K., Daffos, B., Taberna, P.-L., Simon, P., Birkett, G., Zhao, X. S., Holm, C., & Salanne, M. (2016). Capacitance of Nanoporous Carbon-Based Supercapacitors is a Trade-Off Between the Concentration and the Separability of the Ions. *The Journal of Physical Chemistry Letters*, 7(19), 4015–4021.

Chaban, V. V., Andreeva, N. A., & Fileti, E. E. (2018). Graphene/Ionic Liquid Ultracapacitors: Does Ionic Size Correlate With Energy Storage Performance? *New Journal of Chemistry*, 42(22), 18409–18417.

Fatihah, V. A., & Setiarso, P. (2024). The Fabrication of ZnO Nanoparticles-Modified Carbon Paste Electrode for the Analysis of Nicotine Content in E-Cigarette Liquids by Cyclic Voltammetry.

Indonesian Journal of Chemical Research, 12(2), 104–112.

Febriyana, A., & Setiarso, P. (2024). Fabrication of Carbon Paste Electrode Modified with ZnO Nanoparticles and Nanobentonite for Analysis of Bisphenol A by Cyclic Voltammetric. *Indonesian Journal of Chemical Research*, 12(2), 119–128.

Helmholtz, H. (1879). Studien über electrische Grenzschichten. *Annalen Der Physik*, 243(7), 337–382.

IEA. (2024). *Electricity 2024*, *IEA, Paris*. https://www.iea.org/reports/electricity-2024

Inoue, P., Fileti, E., & Malaspina, T. (2020). Computational Study of the Properties of Acetonitrile/Water-in-Salt Hybrid Electrolytes as Electrolytes for Supercapacitors. *The Journal of Physical Chemistry B*, 124(27), 5685–5695.

Ionescu, D., & Kovaci, M. (2024). Prediction of the Specific Energy of Supercapacitors with Polymeric Materials Using Advanced Molecular Dynamics Simulations. *Polymers*, 16(23), 3404.

Jorgensen, W. L., Ghahremanpour, M. M., Saar, A., & Tirado-Rives, J. (2024). OPLS/2020 Force Field for Unsaturated Hydrocarbons, Alcohols, and Ethers. *The Journal of Physical Chemistry B*, 128(1), 250–262.

Li, L., Xu, M., Song, W., Ovcharenko, A., Zhang, G., & Jia, D. (2013). The Effect of Empirical Potential Functions on Modeling of Amorphous Carbon Using Molecular Dynamics Method. *Applied Surface Science*, 286, 287–297.

Neto, A. J. P., & Fileti, E. E. (2018). Differential Capacitance and Energetics of the Electrical Double Layer of Graphene Oxide Supercapacitors: Impact of the Oxidation Degree. *The Journal of Physical Chemistry C*, 122(38), 21824–21832.

Noh, C., & Jung, Y. (2019). Understanding the Charging Dynamics of an Ionic Liquid Electric Double Layer Capacitor: Via Molecular Dynamics Simulations. *Physical Chemistry Chemical Physics,* 21(13), 6790–6800.

Pean, C., Rotenberg, B., Simon, P., & Salanne, M. (2016). Multi-scale Modelling of Supercapacitors: From Molecular Simulations to a Transmission Line Model. *Journal of Power Sources*, 326, 680–685.

Rui, P., Xu, J., Zhao, L., Song, W., Chao, L., Chen, D., & Yang, Z. (2020). Electrolyte Solutions: Measurement and Correlation of the Solubility of Et4NBF4 in Different Solvents at Temperatures from (263.15 to 323.15) K. *International Journal of Electrochemical Science*, 15(10), 10221–10230.

Shuja, A., Khan, H. R., Murtaza, I., Ashraf, S., Abid, Y., Farid, F., & Sajid, F. (2024). Supercapacitors for Energy Storage Applications: Materials, Devices and Future Directions: a Comprehensive Review. *Journal of Alloys and Compounds*, 1009, 176924.

Theodore, A. M., Srivastava, M., Kumar, S., Yahya, M. Z. A., Yadav, T., & Yusuf, S. N. F. (2025). Ionic Liquid Mixed Polymer Electrolyte for Supercapacitor. *Macromolecular Symposia*, 414(1), 1–18.

Wahyuni, W. T., Putra, B. R., Fauzi, A., Ramadhanti, D., Rohaeti, E., & Heryanto, R. (2021). A Brief Review on Fabrication of Screen-Printed Carbon Electrode: Materials and Techniques. *Indonesian Journal of Chemical Research*, 8(3), 210–218.

Wu, X., Liu, Z., Huang, S., & Wang, W. (2005). Molecular Dynamics Simulation of Room-temperature Ionic Liquid Mixture of [bmim][BF4] and Acetonitrile by a Refined Force Field. *Physical Chemistry Chemical Physics*, 7(14), 2771.

Wu, Y., Wu, L., Liu, F., Qiu, Y., Dong, R., Chen, J., Liu, D., Wang, L., & Yi, L. (2024). Molecular Dynamics Simulations Guide the Gasification Process of Carbon-Supported Nickel Catalysts in Biomass Supercritical Water. *Materials*, 17(17), 4192.

Xia, L., Yu, L., Hu, D., & Chen, G. Z. (2017). Electrolytes for Electrochemical Energy Storage. *Materials Chemistry Frontiers*, 1(4), 584–618.

Xu, C., Xu, Z., Wang, Y., Yang, J., Chen, H., Liu, Q., Chen, G., & Yang, H. (2023). Molecular Dynamics Simulation of the Interfacial Structure and Differential Capacitance of [BMI+][PF6−] Ionic Liquids on MoS2 Electrode. *Processes*, 11(2), 380.

Zangi, R. (2018). Refinement of the OPLSAA Force-Field for Liquid Alcohols. *ACS Omega*, 3(12), 18089–18099.